European Geosciences Union General Assembly 2016, EGU
Division Energy, Resources & Environment, ERE

An approach towards a FEP-based model for risk assessment for hydraulic fracturing operations

D. Gläser[a]*, A. Dell'Oca[b], A. Tatomir[c], J. Bensabat[d], H. Class[a], A. Guadagnini[b], R. Helmig[a], C. McDermott[e], M. Riva[b], M. Sauter[c]

[a]*Dept. of Hydromechanics and Modelling of Hydrosystems, University of Stuttgart, Pfaffenwaldring 61, 70569 Stuttgart, Germany*
[b]*Dipartimento di Ingegneria Civile e Ambientale, Politecnico di Milano, Piazza L. Da Vinci 32, 20133 Milano, Italy*
[c]*Dept. of Applied Geology, Geoscience Center, University of Göttingen, Goldschmidtstr. 3, 37077, Göttingen, Germany*
[d] *EWRE Environmental and Water Resources Engineering Ltd., 97a Yefe-Nof St., Haifa 34641, Israel*
e *School of Geosciences, The University of Edinburgh, James Hutton Road, Edinburgh EH9 3FE, United Kingdom*

Abstract

We consider an exemplary scenario drafted in the context of the recently started EU-project FracRisk. The setting belongs to six scenarios representing diverse subsurface processes on different scales. A numerical approach considering sources, pathways and targets quantifies the environmental impact associated with this setting. A Global Sensitivity Analysis of properly defined output quantities takes into account uncertain parameters and operational conditions within a FEP-based evaluation of risk and counteractive measures. At this early stage of the project, this showcase of the general modeling workflow addresses migration of frac-fluid through a naturally fractured reservoir (source) to an overlying formation (target).

Keywords: hydraulic fracturing, global sensitivity analysis, generalized PCE, Sobol indices

* Corresponding author. Tel.: +49 711 685-64624.
  E-mail address: dennis.glaeser@iws.uni-stuttgart.de

1. Introduction

Hydraulic fracturing in combination with unconventional oil or gas production has been implemented extensively primarily in the US in the past ten years. In this operational context, high-pressure injection of fluid into a low-permeability hydrocarbon-bearing formation leads to the formation and (eventually) propagation of new fractures and the enlargement of existing ones. This process makes gas extraction economically feasible. The fluid used for fracturing is typically water mixed with proppants and a variety of chemicals, depending on the characteristics of a considered geological site. The proppants keep the fractures open after the initiation of the fracturing process to ensure that desired flow rates can be achieved. The added chemicals can range from friction reducers to biocides.

Engelder [1] estimates that the Marcellus Shale formation in the Eastern United States will ultimately yield about 14 trillion cubic meters of natural gas with a probability of 50%, where a large number of wells currently extract 312 thousand cubic meters of gas per day [2]. These data are indicative of an impressive economic potential, but concerns have been raised about the environmental impact of the technology, especially with respect to water quantity and quality [3]. The recently started research project FracRisk (funded within the EU Horizon 2020 framework) seeks to identify the potential risks of the technology as well as corresponding mitigation and monitoring strategies. An investigation approach which is well-established in the regulatory risk assessment procedures linking sources (hydrocarbon bearing formation), pathways (e.g. fault zones, abandoned wells) and targets/receptors (e.g. a groundwater reservoir) is used. The approach will be applied to six focused scenarios (see Section 2) in the scope of the project. These scenarios are designed to capture a variety of features, events and processes (FEPs) associated with unconventional gas production. The risk for negative consequences to happen is quantified for each of the scenarios by multiplying the associated probability with the severity. A rigorous sensitivity analysis of certain FEPs on the latter is planned to be performed through detailed numerical modeling. These sensitivities will then be embedded into a FEP-based evaluation of risk and counteractive measures. The collection of data on selected sites across Europe and the USA will ultimately allow the identification of parameter ranges to be employed in the sensitivity analyses, and will provide the needed baseline data for a future application of the monitoring strategies developed in the project.

The main objective of this work is the introduction of a workflow for the determination of parameter sensitivities in the context of the introduced scenario. We illustrate the key steps of the procedure by way of an exemplary showcase (see Section 3). While the latter is not intended as a depiction of a realistic hydraulic fracturing operation, it includes some of the elements of interest in such settings. We describe and test the numerical tools employed in our workflow, which will then be applied to scenario setups associated with an increased level of complexity within the scope of the FracRisk project. A numerical investigation of the environmental impact of hydraulic fracturing can also be found in [4], where numerical simulations were performed for a range of parameters. While the procedure of [4] shares some similarities with ours, we ground our study on a global sensitivity analysis (GSA) where uncertainty is quantified through variance-based Sobol indices (see Section 4). The extensive set of numerical studies and the ensuing probabilistic context within which these are framed in the project will form the core of a robust protocol for risk evaluation.
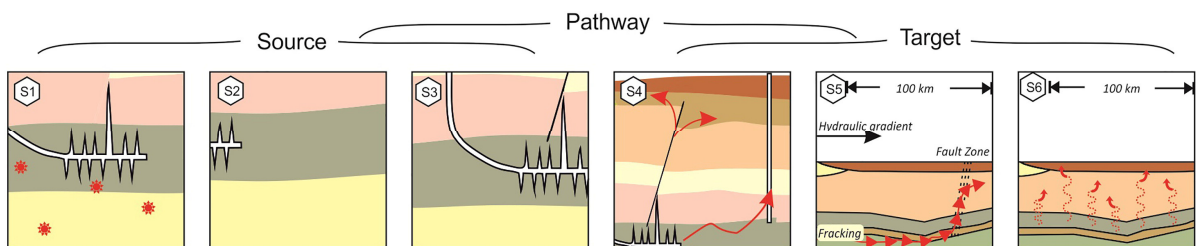

Fig. 1. Illustration of the six focused modeling scenarios considered in Fracrisk. S1: modelling of the fracture growth; S2: Pressure propagation around the fracked source; S3: geochemical modelling; S4: Flow and transport in faults and abandoned wells; S5: Regional transport of displaced fluid; S6: Diffusive transport through the overburden overlying formations and aquifers. Source: www.fracrisk.eu.

2. Focused modeling scenarios for hydraulic fracturing

Scenarios 1-3 of the six focused scenarios considered in FracRisk (see Fig. 1) take a closer look at the source, i.e. the hydrocarbon bearing formation to be fracked, while Scenarios 4-6 consider enlarged spatial and temporal scales and focus on the intermediate- to long-term fate of a contaminant that has escaped from the source rock. Naturally, these scenarios are all interconnected and the results and findings of one of them can be used as an input for others. Scenario 1 attempts to identify the main processes occurring during the fracturing operations, including e.g. the release of gas molecules, formation of pathways or the increase of permeability. Its main focus is on the mechanical description of the hydraulic fracturing process, i.e. the accurate depiction of fracture propagation, the creation of the fracture network and the onset of microseismic events. Findings from this setting can then be embedded into Scenario 2, where the interest is on pressure propagation in the reservoir and on the flow and transport processes through the fracture network and the surrounding porous matrix. The hydrocarbon-bearing formation is represented in detail and the temporal scale of investigation is short. Scenario 3 is an extension of Scenario 2, additionally considering reactive transport phenomena. This will allow investigating the geochemical interactions between the fracturing-fluid components and the reservoir fluids and rock minerals, ultimately leading, e.g., to an assessment of the flow-back composition. Scenario 4 investigates the fate of a potential leakage in the overburden in the presence of, e.g., fault zones or poorly sealed abandoned wells. In comparison to Scenario 4, which considers mid-term processes on the field-scale, Scenario 5 addresses the long-term regional-scale (tens of kilometers) flow and transport of gas, fracturing fluids, or saline water. The last scenario (S6 in Fig. 1) is concerned with long-term (tens of years) diffusive transport of methane through the overburden.

3. Showcase scenario

The showcase scenario we present has been designed to test the feasibility of a general workflow and the associated tools which are developed within the FracRisk project. Based on Scenario 2 (see Section 2), we consider the potential contamination of a target aquifer with a fracturing-fluid component due to high pressure injection of such fluid into an underlying formation (see Fig. 2). Highly conductive pathways through the lower formation are present by means of a fracture network and constitute a direct connection to the target aquifer, i.e. there is no sealing layer between the source and the target. Fluid injection is imposed on a segment of the lower boundary and the overall mass accumulated in the target formation is evaluated at the end of the simulation, i.e. after six hours of injection.

The simple settings of single-phase flow and conservative transport through porous media are considered, as described by the classical system of equations which can be found, e.g., in [8]. A vertex-centered finite volume method (box) is used for the spatial discretization [6], where control volumes are constructed around the grid vertices. The
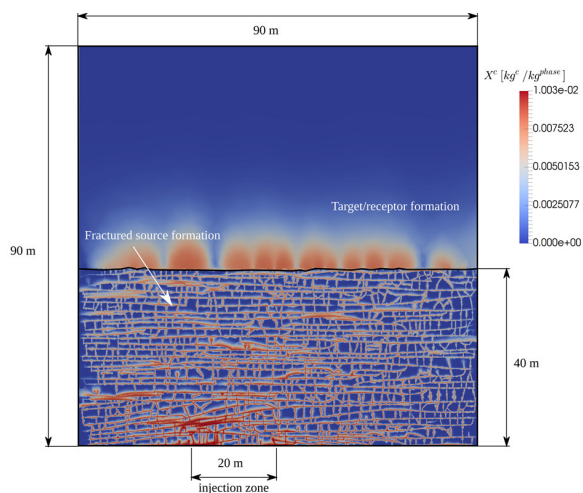

Fig. 2 Snapshot of a simulation result edited to illustrate the model domain, its dimensions and the features included.

conservation equations are integrated over the finite volumes, thus guaranteeing local conservation of the considered quantities. Fluxes are computed on the bounding faces of these control volumes using the finite element basis functions associated with the elements that intersect with the box to evaluate the necessary quantities and their gradients at the flux computation points. The numerical model we employ is an extension of the above described box formulation to account for discrete fractures. Element entities of co-dimension 1 (faces or edges, respectively in in three- or two-dimensions) can herein be identified as fracture entities. In control volumes that are intersected by fracture entities, the flux and storage terms of the system of equations are split into contributions from fracture and matrix, respectively. A detailed description of the computational strategy can be found in [7]. An implicit Euler method has been chosen for the time discretization and the Newton-Raphson method is used to handle the non-linear dependencies of the water-phase density and viscosity on pressure and temperature, for which the IAPWS 97 formulation [5] is employed. For simplicity, the fluid density and viscosity are not considered to depend on the concentration of the transported component. The numerical model is implemented in the free open-source numerical simulator DuMu^x [8] and can handle two- and three-dimensional settings. Here, we focus on a two-dimensional showcase.

The fracture network as an input for the simulations can be obtained from measurements or by using a geostatistical fracture network creator, as e.g. Frac3D [9, 10]. The resulting two- or three-dimensional geometries can be meshed using, e.g., Art3D [11] or Gmsh [12]. As we do not solve for the geomechanical deformations of the host rock in our model, fracture propagation is not simulated and the fracture network is assumed to be static throughout the entire simulation. The fracture network geometry for this showcase has been obtained from a scan of a limestone outcrop in Bristol [13, 14], scaled by a factor of five. Even though it is not completely representative for shale, the resulting geometrical pattern has been chosen to illustrate that the numerical model is not bound by any geometrical constraint.

The injection length of approximately 20 m on the domain lower boundary (see Fig. 2) is designed to represent a stage of a hydraulic fracturing operation. Injection occurs at five discrete positions representing the perforated parts of the stage. These five injection points were chosen to coincide with intersections of fractures with the boundary to ensure the largest possible injection rate feeding directly into the fracture network. The injection is simulated by a Cauchy-type boundary condition, where the pressure at the boundary, p_{inj}, is specified and the resulting mass flux into the domain is calculated via:

$$q_{inj} = -a_f \rho_w(p_{inj}) \frac{\mathbf{K}_f}{\mu_w(p_{inj})} \left(\frac{\mathbf{x}_{inj} - \mathbf{x}_f}{\| \mathbf{x}_{inj} - \mathbf{x}_f \|^2} \left(p_{inj} - p_f \right) - \bar{\rho}_w \mathbf{g} \right) \mathbf{n}. \tag{1}$$

Here, $\mathbf{K}_f$ is the intrinsic permeability tensor of the fracture, p_f is the actual pressure in the fracture, $\mathbf{x}_{inj}$ is the position of the injection point, i.e. the intersection of a fracture with the boundary, $\mathbf{x}_f$ is the center of the fracture entity with aperture a_f, $\mathbf{g}$ is the gravitational acceleration and $\mathbf{n}$ is the unit outer normal vector of the boundary face. The averaged water phase density $\bar{\rho}_w = (\rho_w(p_{inj}) + \rho_w(p_f))/2$ is used to evaluate gravitational forces in Equation (1). A fully-upwind approach is applied for the calculation of density ρ_w and viscosity μ_w in Equation (1). For the transport equation of the component the boundary influx q_{inj} has to be multiplied by the specified concentration of the component in the fluid to be injected. This has been set to $X^c = 0.01$. Neumann no-flow conditions are set along the remaining segments of the lower boundary, as well as on the two lateral boundaries. A hydrostatic pressure distribution and a zero solute concentration were applied as initial conditions and Dirichlet boundary conditions on the upper boundary. A constant geothermal gradient of 30 K/km has been assumed to drive the temperature distribution.

We note that the scenario setup at this early stage of the project is not a truly realistic representation of an actual hydraulic fracturing operation. For example, the fracture network geometry, obtained from a limestone, does not represent a shale formation in all its details. Furthermore, the pattern of the fracture network does not evolve during the simulations but is considered to be already fully developed prior to the injection. Reducing the system to two dimensions and imposing no-flow boundaries on the lateral sides contribute to an overestimation of the pressure and, thus, to increased flow rates being transmitted towards the target formation. The absence of a sealing layer above the source rock and the relatively long injection time of six hours further increase the likelihood and the level of a contamination within the target aquifer. However, it is also noted that this showcase has not been designed to actually evaluate the potential risks of the technology, which is a final aim of the project. As stated above, it aims at providing a preliminary testing of the workflow and of the simulation/analysis tools involved. More realistic setups will be

created and a larger set of parameters are expected to be included in the sensitivity analysis for the actual modeling of the scenarios within the project.

Table 1 Parameter choices used for the showcase

Parameter	Unit	Value
Fracture aperture a_f	m	$[1 \times 10^{-5} - 1 \times 10^{-3}]$
Injection pressure p_{inj}	bar	$[150 - 350]$
Intrinsic permeability of the target formation $\mathbf{K}_{TA}$	m^2	$[1 \times 10^{-11} - 1 \times 10^{-13}]$
Intrinsic permeability of the source matrix $\mathbf{K}_S$	m^2	1×10^{-14}
Intrinsic permeability of the source fractures $\mathbf{K}_F$	m^2	1×10^{-8}
Porosity of the target formation Φ_{ta}	-	0.25
Porosity of the source matrix Φ_s	-	0.1
Porosity of the source fractures Φ_f	-	0.7

4. Sensitivity Analysis

In this study, as output quantity of interest we focus on the accumulated mass of contaminant in the target aquifer, Ω_{TA}, at the end of the injection period

$$\overline{\mathrm{M}} = \int_{\Omega_{TA}} \rho_w X^c \Phi_{TA} d\Omega_{TA}. \tag{2}$$

We investigate the sensitivity of $\overline{\mathrm{M}}$ with respect to the three parameters $\mathbf{K}_{TA}$, a_f, and p_{inj}. The first two of these represent our lack of knowledge about aquifer properties, whereas p_{inj} represents the effect of varying operational conditions. We consider only three parameters in this work, because the main focus is to test the applicability of the GSA described in the following to the highly non-linear problem at hand. We perform a GSA grounded on variance-based Sobol indices (see e.g. [15, 16]). Sobol indices provide a measure of the amount of the total variance of an output quantity of interest that can be ascribed to uncertainty/variability of each of the uncertain input parameters. Here, we briefly recall the main steps that lead to the evaluation of Sobol indices through a generalized Polynomial Chaos Expansion (gPCE). Further details can be found e.g. in [17] and references therein. The parameters $\mathbf{K}_{TA}$, a_f, and p_{inj} are collected in vector $\mathbf{x} = (x_1,...,x_N)$, where $N = 3$. Since no prior information is available at this stage, we assume each x_n to be uniformly distributed within the interval $\Gamma_n = \left[x_{n,\min}, x_{n,\max} \right]$ (see Table 1). The joint probability of the input parameters is $\rho_\Gamma(\mathbf{x}) = \prod_{i=1}^{N}(x_{i,\max} - x_{i,\min})^{-1}$ since we consider them statistically independent. The accumulated mass in the target aquifer is expressed in terms of a gPCE, which can be cast as

$$\overline{\mathrm{M}}(\mathbf{x}) \simeq \beta_0 + \sum_{i=1}^{N} \sum_{\mathbf{p} \in \mathfrak{I}_i} \beta_{\mathbf{p}} \psi_{\mathbf{p}}(\mathbf{x}) + \sum_{i=1}^{N} \sum_{j=1}^{N} \sum_{\mathbf{p} \in \mathfrak{I}_{i,j}} \beta_{\mathbf{p}} \psi_{\mathbf{p}}(\mathbf{x}) + ...,$$

$$\psi_i(\mathbf{x}) = \prod_{i=1}^{N} \psi_{i,p_i}(x_i), \quad \beta_{\mathbf{p}} = \int_{\Gamma} M(\mathbf{x}) \psi_i(\mathbf{x}) \rho_\Gamma(\mathbf{x}) d\mathbf{x}, \tag{3}$$

where $\mathbf{p} = \left\{ p_1,..., p_N \right\} \in \mathbb{N}^N$ is a multi-index expressing the degree of each univariate Legendre polynomial, $\psi_{i,p_i}(x_i)$, employed to construct the multivariate orthonormal Legendre polynomial $\psi_i(\mathbf{x})$ (see [18]), $\beta_{\mathbf{p}}$ is the associated gPCE coefficient and $\mathfrak{I}_i$ contains all indices such that only the ith component does not vanish, i.e. $\mathfrak{I}_i = \left\{ p_i \neq 0, p_k = 0 \, for \, k \neq i \right\}$. Note that β_0 represents the mean of $\overline{\mathrm{M}}$, $\mu_{\overline{\mathrm{M}}}$. From a practical perspective, the series in Equation (3) are truncated to save computational time. In this work, we select a total-degree rule, i.e. $\sum_i p_i \leq w$ [19], the accuracy of gPCE increasing with w. Equation (3) is equivalent to the ANOVA decomposition [20]. The full set of Sobol indices can then be computed as

$$S_{i_1,\dots,i_s} = \frac{1}{V_{\overline{M}}} \sum_{p \in \mathfrak{I}_{i_1,\dots,i_s}} \beta_p^2, \quad V_{\overline{M}} = \sum_{p \in \mathbb{N}^N} \beta_p^2 - \beta_0^2, \tag{4}$$

$V_{\overline{M}}$ being the total variance of $\overline{M}$. The Sobol indices $S_{i_1,\dots,i_s}$ quantify the relative contributions to $V_{\overline{M}}$ ascribed to a mixed effect of $x_1,\dots,x_s$. The principal Sobol index of the ith parameter, S_i, and the total Sobol index are defined as

$$S_i = \frac{1}{V_{\overline{M}}} \sum_{p \in \mathfrak{I}_i} \beta_p^2, \qquad S_i^T = S_i + \sum_j S_{i,j} + \sum_{k,j} S_{i,j,k} + \dots \tag{5}$$

The former quantifies the contribution of the ith parameter alone to $V_{\overline{M}}$, while the total Sobol index also includes contributions due to interaction of the ith parameter with other parameters. The coefficients β_p are calculated by solving the multidimensional integral in Equation (3) through a sparse grids interpolation technique [17]. The full system model introduced in Section 3 is used to solve the flow and transport problems driven by parameter values corresponding to the coordinates of the collocation points of the sparse grid spanning the parameter space. An additional benefit of the workflow is that a gPCE representation constitutes a surrogate (or reduced complexity) model of the target environmental quantity, $\overline{M}$. As such, having at our disposal the gPCE enables us to perform a complete probabilistic analysis of the system state without the need of multiple evaluations of the full system model. This would result in a considerable saving of computational time. Due to the nature of this work, this aspect is not completely explored here.
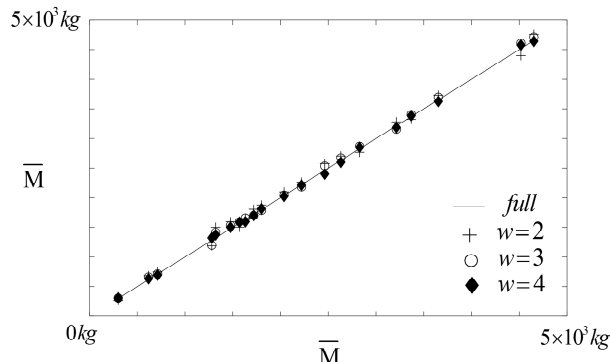

Fig. 3. Scatter plot of the total accumulated mass of contaminant in the target aquifer ($\overline{M}$) obtained by the full model (horizontal axis) vs. the corresponding gPCE representations (vertical axis) associated with total degree $w = 2$, crosses; $w = 3$, circles; $w = 4$, diamonds. The continuous line of slope 1/1 is included as a reference.

5. Results

We present here the results of the GSA described in Section 4. We study the quality of the gPCE representations of $\overline{M}$ by drawing randomly 20 parameter combinations from Γ and comparing the results obtained from (a) the full numerical model described in Section 3 against those of (b) a gPCE representation for $w = 2$, 3, and 4. Fig. 3 depicts a scatterplot of values of $\overline{M}$ obtained through the full model solution and a gPCE of total order $w = 2$, 3, and 4. These results imbue us with confidence that a gPCE of order $w \geq 2$ yields results of acceptable quality for the setting considered. Table 2 lists values of the mean, $\mu_{\overline{M}}$, variance, $V_{\overline{M}}$, coefficient of variation, $CV_{\overline{M}} = V_{\overline{M}}^{0.5} / \mu_{\overline{M}}$, and principal and total Sobol Indices S_n and S_n^T (for $n = K_{TA}$, a_f, p_{inj}) of $\overline{M}$ for $w = 2$, 3, and 4. An inspection of the results listed in Table 1 suggests that the investigated statistical moment of $\overline{M}$ and the associated principal and total Sobol indices can be considered to be convergent with respect to the gPCE order, i.e. the total degree w. In the

following we will show results for $w = 4$. Analysis of $S_{K_{TA}}$ and $S_{K_{TA}}^T$ suggests that the uncertainty affecting K_{TA} practically does not contribute to the output variance $V_{\overline{M}}$. Instead, the major contribution to $V_{\overline{M}}$ is associated with a_f. This can be seen by inspection of S_{a_f} and $S_{a_f}^T$ and indicates that the uncertainty in the fracture aperture contributes to more than seventy per cent of the output variance. Close inspection of $S_{p_{inj}}$ and $S_{p_{inj}}^T$ suggests that more than twenty per cent of the output variance is governed by the variability of p_{inj}. It is also noted that the principal and total Sobol indices values are relatively close, indicating a small level of interaction between the uncertain parameters considered.

Table 2 Mean, $\mu_{\overline{M}}$, variance, $V_{\overline{M}}$, coefficient of variation, $CV_{\overline{M}}$, principal and total Sobol Indices S_i and S_i^T associated with gPCE of total order $w = 2, 3, 4$.

	$w = 2$	$w = 3$	$w = 4$
$\mu_{\overline{M}}$ [Kg]	2.28×10^3	2.25×10^3	2.23×10^3
$V_{\overline{M}}$ [Kg^2]	2.63×10^6	2.40×10^6	2.27×10^6
$CV_{\overline{M}}$	0.71	0.69	0.68
$S_{K_{TA}}$	1.88×10^{-6}	1.03×10^{-5}	9.09×10^{-5}
S_{a_f}	0.696	0.690	0.713
$S_{p_{inj}}$	0.246	0.247	0.231
$S_{K_{TA}}^T$	2.415×10^{-6}	4.27×10^{-5}	2.52×10^{-4}
$S_{a_f}^T$	0.754	0.753	0.769
$S_{p_{inj}}^T$	0.304	0.310	0.287

6. Summary and Outlook

An approach for the assessment of parameter sensitivities, to be embedded into a FEP-based risk assessment of hydraulic fracturing operations, has been presented on an exemplary showcase. The latter considers a naturally fractured reservoir into which the injection of a fluid carrying a potentially hazardous component leads to a contamination in an overlying aquifer (target). Contamination is quantified through the total mass of the component accumulated in the target and model sensitivities with respect to a set of uncertain model input parameters are quantified.

The presented approach using a GSA grounded on variance-based Sobol indices evaluated through a gPCE representation of the full system model. The main advantage of this approach is that it can quantify the dependency of the variance of an output quantity on the uncertainty of an input parameter as well as on cross dependencies on multiple input parameters. The current work is intended as a preliminary step towards an extensive investigation of the potential environmental impact of hydraulic fracturing. In this sense, the procedure introduced is key for investigating all six focused modeling scenarios defined in the FracRisk project, in the presence of diverse uncertain parameters. This detailed study will be carried out within the scope of the project together with the development of a FEP-based model for risk assessment.

Acknowledgements

References

[1] Engelder T. Marcellus. *Fort Worth Basin Oil and Gas Magazine* 2009;18-22.

[2] U.S. Energy Information Administration. Drilling Productivity Report, May 2016. http://www.eia.gov/petroleum/drilling/

[3] Entrekin S, Evans-White M, Johnson B, Hagenbuch E. Rapid expansion of natural gas development poses a threat to surface waters. *Frontiers in Ecology and the Environment* 2011;9:503-511.

[4] Reagan MT, Moridis GJ, Keen ND, Johnson JN. Numerical simulation of the environmental impact of hydraulic fracturing of tight/shale gas reservoirs on near-surface groundwater: Background, base cases, shallow reservoirs, short-term gas, and water transport. *Water Resour. Res* 2015;51:2543-2573.

[5] Wagner W, Cooper JR, Dittmann A. The IAPWS Industrial Formulation 1997 for the Thermodynamic Properties of Water and Steam. *Journal of Engineering for Gas Turbines and Power* 2000;122(1):150-184.

[6] Helmig R. *Multiphase flow and transport processes in the subsurface: a contribution to the modeling of hydrosystems*. Springer-Verlag; 1997.

[7] Tatomir A. From discrete to continuum concepts of flow in fractured porous media. PhD thesis, *Universitätsbibliothek der Universität Stuttgart* 2012.

[8] Flemisch B, Darcis M, Erbertseder K, et al. DuMux: DUNE for multi-{phase, component, scale, physics, …} flow and transport in porous media. *Advances in Water Resources* 2001;34:1102–1112.

[9] Assteerawat A. Flow and transport modelling of fractured aquifers based on a geostatistical approach. PhD thesis, *Universitätsbibliothek der Universität Stuttgart* 2008.

[10] Silberhorn-Hemminger A. Modellierung von Kluftaquifersystemen. Geostatistische Analyse und deterministisch stochastische Kluftgenerierung. PhD thesis, *Universitätsbibliothek der Universität Stuttgart* 2013.

[11] Fuchs A. Almost regular triangulation of trimmend nurbs-solids. *Engineering with Computers* 2001;17(1):1102-1112.

[12] Geuzaine C, Remacle J-F. Gmsh: a three-dimensional finite element mesh generator with built-in pre- and post-processing facilities. *International Journal for Numerical Methods in Engineering* 2009;79(11):1309-1331.

[13] Belayneh M, Geiger S, Matthai SK. Numerical simulation of water injection into layered fractured carbonate reservoir analogs. *AAPG Bulletin* 2006;90:1473-1493.

[14] Tatomir A, Szymkiewicz A, Class H, Helmig R. Modeling two phase flow in large scale fractured porous media with an extended multiple interacting continua method. *CMES - Computer Modeling in Engineering and Sciences* 2011;77:81-111.

[15] Sobol IM. Sensitivity estimates for nonlinear mathematical models. *Math Model Comput Exp* 1993;1:407-17.

[16] Archer GEB, Saltelli A, Sobol IM. Sensitivity measures, anova-like techniques and the use of bootstrap. *J Stat Comput Simul* 1997;58:99-120.

[17] Formaggia L, Guadagnini A, Imperiali I, Lever V, Porta G, Riva M, Scotti A, Tamellini L. Global sensitivity analysis through polynomial chaos expansion of a basin-scale geochemical compaction model. *Comput Geosci* 2013;17:25-42.

[18] Gautschi W. Orthogonal polynomials: computation and approximation. *Oxford University Press* 2004.

[19] Bäck J, Nobile F, Tamellini L, Tempone R. Stochastic spectral Galerkin and collocation methods for PDEs with random coefficients: a numerical comparison. In: Hesthaven JS, Ronquist EM editors. *Lecture notes in computational science and engineering. Spectral and high order methods for partial differential equations*. Berlin Heidelberg: Springer-Verlag; 2011, p. 43-62.

[20] Sudret B. Global sensitivity analysis using polynomial chaos expansions, *Reliab. Eng. Syst. Safety* 2008;93(7), 964-979.